DOI: 10.1002/ejic.200900708

Neutral and Cationic Hydridoruthenium Tetrakiscarbene Complexes

Robert Wolf,*[a] Markus Plois,[a] and Alexander Hepp[a]

Keywords: Ruthenium / Hydrides / Carbene ligands

Starting from the novel chlorido precursor *trans*-[$RuCl_2$-(IMe)$_4$] (**1**, IMe = 1,3,4,5-tetramethylimidazol-2-ylidene), hydridoruthenium complexes *trans*-[RuH_2(IMe)$_4$] (**2**) and [RuH-(IMe)$_4$][BEt_4] (**3**BEt_4) have been synthesized. Complex **2** was isolated from the reaction of **1** with $LiAlH_4$, while ionic compound **3** was obtained when $LiBHEt_3$ was used as the hydride source. Complexes **1**–**3** have been characterized by X-ray crystallography, multinuclear NMR, IR, UV/Vis spectroscopy and mass spectrometry. Neutral dihydride **2** displays a tetragonal bipyramidal geometry with four carbene groups coordinated to ruthenium in equatorial positions and two apical hydrogen atoms. DFT calculations suggest that the *trans* structure observed for **2** is preferred over a *cis* arrangement for steric reasons. The ruthenium atom of **3** has a tetragonal pyramidal coordination environment with a vacant coordination site sterically protected by the Me substituents of the ligands. Thus, compound **3** should be an attractive target for future coordination studies.

Introduction

Hydridoruthenium complexes [RuH_2L_4] and [$RuHL_4$]$^+$ bearing mono- to tetradentate phosphane ligands (L) catalyze a variety of organic transformations,[1,2] and their ability to bind dihydrogen and other small molecules, for example O_2 and N_2, is noteworthy.[1,3] The synthetic utility of such complexes is further illustrated by the recent stabilization of the cyaphide anion (C≡P$^-$), end-on coordinated in the complex [RuH(CP)(dppe)$_2$] [dppe = 1,2-bis(diphenylphosphanyl)ethane].[4] Replacing phosphanes by N-heterocyclic carbenes (NHCs) should significantly alter the steric and electronic properties of the resulting complexes,[5] with a beneficial impact on potential applications in catalysis and small molecule activation. Various hydridoruthenium complexes containing NHCs have been reported some of which are active catalysts. Among other reactions, NHC hydridoruthenium complexes catalyze the hydrodefluorination of fluorinated arenes and the tandem dehydrogenation/Wittig reaction.[6] Ín addition, these reactive compounds often show a marked propensity for the activation of ligand C–H bonds[7] while C–C or C–N bond activations have also been observed.[7b,8]

The vast majority of hydridoruthenium complexes containing NHCs display additional ancillary ligands such as carbon monoxide or halides. Compounds that *exclusively* contain NHCs next to the hydrido ligands are exceedingly rare.[9] A very recent report of the complex [RuH(IPrMe$_2$)$_4$]$^+$ (IPrMe$_2$ = 1,3-diisopropyl-4,5-dimethylimidazol-2-ylidene)[9b,9c] by Whittlesey and co-workers now prompts us to disclose our own, independent results in this area. Here we report the synthesis and characterization of two novel tetrakiscarbene hydrido complexes, *trans*-[RuH_2(IMe)$_4$] (**2**, IMe = 1,3,4,5-tetramethylimidazol-2-ylidene) and [RuH-(IMe)$_4$][BEt_4] (**3**BEt_4), which have been prepared from the new chlorido complex *trans*-[$RuCl_2$(IMe)$_4$] (**1**).

Results and Discussion

Syntheses of 1–3

The chlorido complex *trans*-[$RuCl_2$(IMe)$_4$] (**1**) was initially obtained as an air-sensitive, orange-brown solid from the reaction of [$RuCl_2(PPh_3)_3$] with four equivalents IMe. Unfortunately, the separation from the triphenylphosphane by-product proved to be cumbersome. Subsequently, we found that **1** can be prepared in excellent purity by heating IMe (four equivalents) with [$RuCl_2$(cod)]$_x$ in toluene for several hours (Scheme 1).

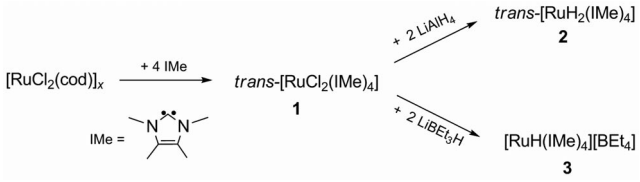

Scheme 1. Syntheses of **1**–**3**.

Targeting new hydridoruthenium carbene complexes, we reacted **1** with hydride sources. First, we examined the reaction with a slight excess of $LiAlH_4$. Gratifyingly, we ob-

[a] Universität Münster, Institut für Anorganische und Analytische Chemie,
Corrensstr. 30, 48149 Münster, Germany
E-mail: r.wolf@uni-muenster.de
http://www.uni-muenster.de/Chemie.ac/uhl/wolf.html

Supporting information for this article is available on the WWW under http://dx.doi.org/10.1002/ejic.200900708.

tained the yellow target complex *trans*-[$RuH_2(IMe)_4$] (**2**), which could be characterized by an X-ray crystal structure analysis (vide infra). NMR spectroscopic investigations of the isolated solid reproducibly showed the presence of varying amounts of a second species which was extremely difficult to separate from **2**. It seems likely that this by-product, which was characterized by ^1H and ^{13}C NMR spectroscopy, is the intermediate chlorido complex [RuHCl$(IMe)_4$]. Although repeated attempts to modify the synthetic procedure by using a large excess of $LiAlH_4$, longer reaction times or heating failed to give pure **2**, the contamination with the by-product can be limited to approximately 20% (according to ^1H NMR spectroscopy) by adding $LiAlH_4$ in a sequential fashion.

When dichlorido complex **1** was treated with $LiBHEt_3$ the reaction took a completely different course. The reaction mixture assumed a deep violet color immediately on addition of the hydride reagent, and the ionic complex [RuH$(IMe)_4$][BEt_4] (**3**BEt_4) was isolated. Thus, one of the chlorine atoms of **1** is exchanged for a hydrogen while the second chlorine is eliminated, presumably as lithium chloride. The observation of the $[BEt_4]^-$ anion in **3**BEt_4 may at first seem surprising. However, this anion has previously been observed several times in reaction mixtures involving "super-hydride" $LiBHEt_3$.[10,11] Its formation may be explained by an equilibrium formed between BEt_3, $LiBHEt_3$, $LiBEt_4$ and $(BHEt_2)_2$ in the reaction mixtures.[10h]

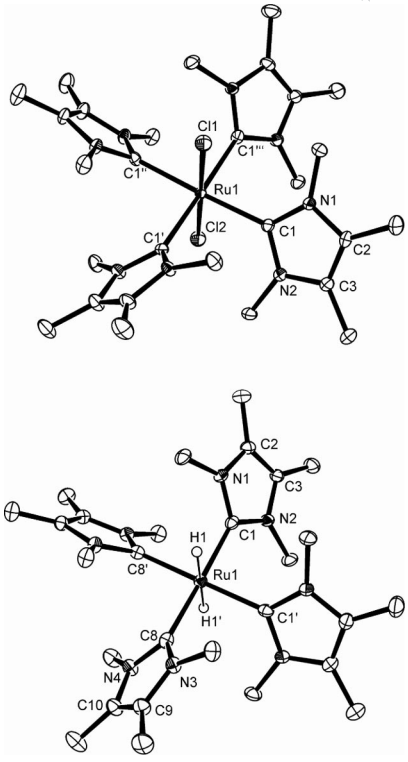

Figure 1. Solid-state molecular structures of *trans*-[$RuCl_2(IMe)_4$] (**1**, top) and *trans*-[$RuH_2(IMe)_4$] (**2**, bottom, thermal ellipsoids at 40% level, H-atoms not shown except for H1 and H1′ of **2**); symmetry transformations used to generate equivalent atoms of **1**: ′ $-y + 1, x + 1, z$; ′′ $y -1, -x + 1, z$; ′′′ $-x, -y + 2, z$; of **2**: ′ $-x + 3/4, -y + 3/4, z$.

Single-Crystal X-ray Structures

Single-crystal X-ray structure analyses of **1**–**3** have been carried out at –120 °C. Complex **1** crystallizes in the tetragonal space group *P*4*nc* with two molecules in the unit cell. The molecules reside on a crystallographic C_4 axis and display a square-bipyramidal coordination of ruthenium by four IMe ligands and two chlorine atoms in a *trans* arrangement (Figure 1). The rather long ruthenium–carbon and ruthenium–chlorine distances [Ru1–C1 2.113(2) Å, Ru1–Cl1 2.465(2) Å, Ru1–Cl2 2.516(2) Å, Table 1] may be caused by the repulsion between the chlorine atoms and the methyl substituents at nitrogen which are only 3.213 Å apart.[12,13] The carbene ligands are tilted with respect to the Cl–Ru–Cl axis (torsion angle Cl1–Ru1–C1–N1 –39.4°). Long Ru–Cl and Ru–C distances [Ru–Cl 2.455(3), 2.463(3) Å, Ru–C 2.103(9)–2.111(9) Å] have been reported by Lappert et al. for the related complex *trans*-[$RuCl_2L_4$] (L = 1,4-diethylimidazol-2-ylidine), which also displays similar Cl–Ru–C–N torsion angles (–38.24 to –44.44°) as **1**.[14]

Dihydrido complex **2** crystallizes in the orthorhombic space group *Fddd* with 16 formula units per unit cell (Figure 1). The individual molecules are located on crystallographic C_2 axes and display a tetragonal bipyramidal arrangement of four carbenes and two *trans*-coordinated hydrido ligands similar to the structure of **1**. Within the accuracy of the X-ray diffraction experiment, the Ru1–H1 distance of 1.69(3) Å is in the range of values observed for other hydridoruthenium complexes.[1,15,16] The Ru–C bond lengths of 2.064(2) to 2.058(2) Å are in the normal range (Table 1).[16] Similar to **1**, the carbene ligands are tilted with respect to the H–Ru–H axis (H1–Ru1–C1–N1 –42.3°, H1–Ru1–C8–N8 –44.0°).

Deep violet **3**BEt_4 crystallizes in the orthorhombic space group *Pcca* with four molecules in a unit cell. The compound displays an ion-separated structure which consists of the $[RuH(IMe)_4]^+$ cation (**3**) and the $[BEt_4]^-$ anion (Figure 2). Both anion and cation reside on crystallographic C_2 axes. The ruthenium atom is coordinated in a pyramidal fashion by the four equatorial carbenes and one apical hydrogen atom. The metal center is located perfectly in the plane spanned by the four carbene carbon atoms. The Ru–H distance [Ru1–H1 1.62(3) Å] is identical to that in **2** within the accuracy of the experiment. The Ru–C bonds are only marginally longer than in **2** (Table 1). As for the structures of **1** and **2**, a "propeller-like" arrangement of the NHC ligands is observed (H–Ru–C–N range 28.1–43.3°). The steric crowding induced by the carbene ligands becomes apparent from van-der-Waals structure of cation **3** (Figure 3). Four carbene methyl groups create a sterically shielded "coordination pocket" around the vacant coordination site of ruthenium. Nevertheless, this space-filling model also indicates that the metal center still ought to be accessible for small donor molecules (Figure 2).[17] The $[BEt_4]^-$ anion displays normal structural parameters.[10,18]

Table 1. Selected bond lengths [Å] and angles [°] of **1**, **2** and **3**BEt_4 (values calculated at the DFT BP86-D/def2-TZVP level for **2** and cation **3** are given in parentheses, symmetry transformations used to generate equivalent atoms in the X-ray structures of **1**: $'$ $-y + 1, x + 1, z$; $''$ $y - 1, -x + 1, z$; $'''$ $x, -y + 2, z$; of **2**: $'$ $-x + 3/4, -y + 3/4, z$; of **3**: $'$ $-x + 1/2, -y, z$.

	1		**2**	**3**BEt_4
Ru1–Cl1	2.465(2)	Ru1–H1	1.69(3) [1.707]	1.62(3) [1.556]
Ru1–Cl2	2.516(2)	Ru1–C1	2.058(2) [2.036]	2.0729(13) [2.055]
Ru1–C1	2.113(2)	Ru1–C8	2.064(2) [2.036]	2.0896(13) [2.058]
C1–N1	1.376(3)	C1–N1	1.378(3) [1.384]	1.3725(17) [1.374]
C1–N2	1.376(3)	C8–N3	1.379(3) [1.384]	1.3699(16) [1.376]
C2–N1	1.396(3)	C1–N2	1.379(3) [1.384]	1.3962(16) [1.378]
C3–N2	1.396(3)	C8–N4	1.380(3) [1.384]	1.3677(17) [1.377]
C2–C3	1.338(4)	C2–N1	1.395(3) [1.396]	1.3737(16) [1.395]
Cl1–Ru1–Cl2	180.000(1)	C10–N3	1.394(3) [1.396]	1.3945(17) [1.396]
C1–Ru1–Cl2	92.07(10)	C3–N2	1.400(3) [1.396]	1.350(2) [1.396]
C1–Ru–Cl1	87.93(10)	C9–N4	1.397(3) [1.396]	1,3938(17) [1.395]
C1–Ru–C1′	175.9(2)	C2–C3	1.344(3) [1.366]	1.3968(17) [1.367]
		C9–C10	1.345(3) [1.366]	1.3457(19) [1.367]
		C1–Ru1–H1,	89.2(9) [90.0]	88.31 [87.7]
		C8–Ru1–H1	89.3(9) [90.0]	89.0(9) [91.7]
		C1–Ru–C1′	87.47(11) [90.0]	99.07(7) [93.9]
		C1–Ru1–C8	178.13(8) [180.0]	86.40(5) [86.2]
		B1–C103	–	165.5(2)
		B1–C101	–	165.3(2)
		C–B1–C range	–	107.47(17)–110.85(8)

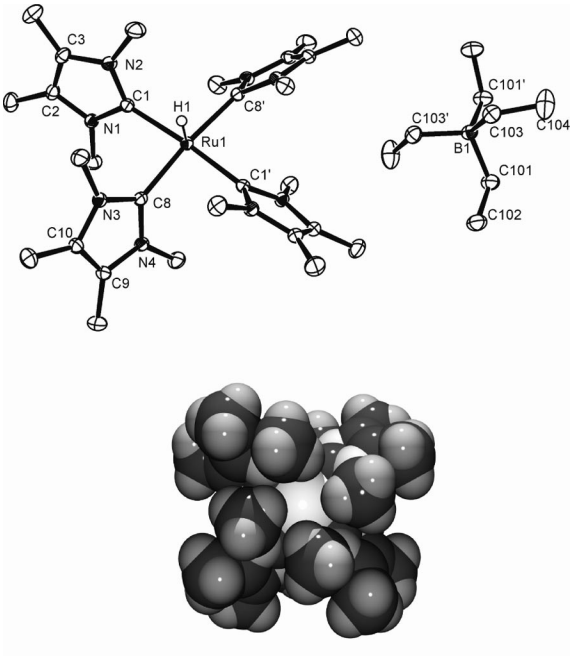

Figure 2. Top: solid-state molecular structure of $[RuH(IMe)_4][BEt_4]$ (**3**BEt_4, thermal ellipsoids at 40% level, disorder of H1 and H-atoms bound to carbon not shown). Bottom: space-filling model of cation **3**; symmetry transformations used to generate equivalent atoms of **3**: $'$ $-x + 1/2, -y, z$.

Spectroscopic Characterization

The molecular ions could not be detected in the mass spectra of **1**–**3**, but characteristic fragments have been observed which are in agreement with the assigned structures. In particular, the MALDI spectra of **2** and **3** showed dominant peaks for the $[RuH(IMe)_4]^+$ cation. In the infrared spectrum, the Ru–H stretch of dihydrido complex **2** was observed at 1852 cm^{-1}. A smaller absorption at 1713 cm^{-1} may be assigned to the presumed by-product $[RuHCl(IMe)_4]$. For cation **3**, the Ru–H stretch is shifted to higher wavenumbers (2081 cm^{-1}). Similar values have been reported for $[RuH_2(dippe)_2]$ and $[RuH(dippe)_2][BPh_4]$, respectively.[3]

Multinuclear NMR spectroscopic studies fully support the structural assignments of **1**–**3**. The ^{13}C NMR signals of the carbene carbons coordinated to ruthenium are in the usual range (**1**: 198.7 ppm, **2**: 212.0 ppm, **3**: 200.9 ppm).[2] Only one set of methyl resonances was detected for **1** and **2** with chemical shifts similar to those observed for the free carbene IMe. Dihydride **2** showed a hydride resonance at δ = –7.45 ppm in the ^1H NMR spectrum. Similar shifts have recently been reported by Milstein et al. for *trans*-dihydridoruthenium complexes containing PONOP pincer ligands.[19] The minor by-product observed in the synthesis of **2** featured a hydride resonance of –16.24 ppm and two sets of Me signals in the ^1H NMR spectrum, indicating the reduced symmetry of this complex. The $^{13}C\{^1H\}$ spectrum revealed a shift of 200.9 ppm for the carbene C atom, an identical value as for cationic **3**.

The ^1H NMR spectrum of **3**BEt_4 in non-coordinating fluorobenzene showed a hydride signal at –39.06 ppm, similar to the high-field shifts reported for $[RuH(IPrMe_2)_4][BAr^F_4]$ (δ = –41.2 ppm) and $[RuH(dippe)_2][BPh_4]$ [δ = –31.0 ppm, dippe = 1,2-bis(diisopropyl)phosphanylethane].[3,9] Broad multiplets at δ = 0.94 and 1.58 ppm, and a broad ^{11}B NMR resonance at –16.5 ppm ($[D_8]$THF) confirmed the presence of the tetraethylborate anion.[10,11] Variable-temperature ^1H NMR spectra of **3**BEt_4 in coordinating $[D_8]$THF down to –50 °C point to the formation of a rapid equilibrium between the free $[RuH(IMe)_4]^+$ cation (**3**) and the THF adduct $[RuH(IMe)_4([D_8]thf)]^+$ (**3**thf),

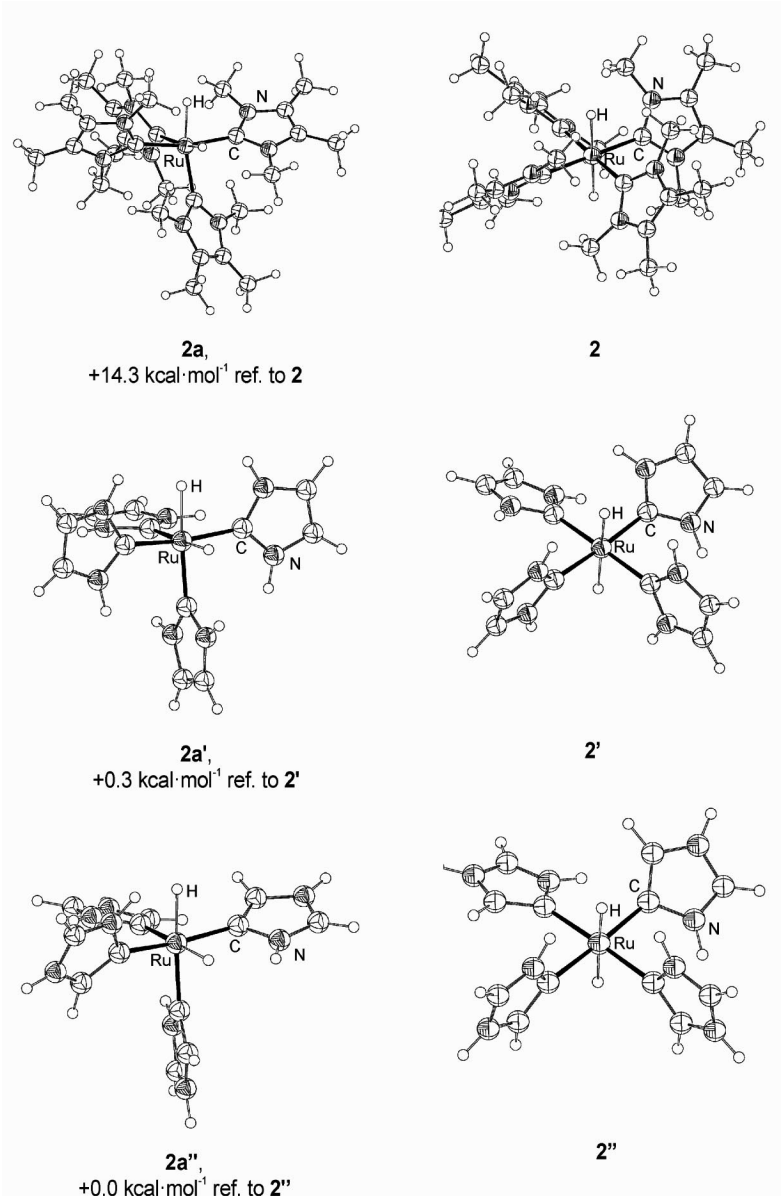

Figure 3. Optimized structures of tetrakiscarbene hydridoruthenium complexes.

which are present in a ratio of 6:1 at –50 °C. A high-field singlet at –40.01 ppm may be assigned to **3** while a second signal in the hydride region at –8.99 ppm arises from the adduct **3**thf.[20] The carbene resonances of **3** and **3**thf showed partial overlap. A NOESY spectrum recorded at –50 °C revealed exchange cross peaks between both species. An NOE was observed between the pair –40.01/3.13 ppm (hydride/*N*-Methyl signal of the free cation **3**), demonstrating that the corresponding hydrogen atoms are in close proximity. Similarly, the N-methyl signal of **3**thf at δ = 3.03 ppm showed an NOE with the hydride signal at –8.99 ppm. At room temperature in [D_8]THF, only a very broad peak at –40.1 ppm was observed for **3** due to partial coalescence with the hydride signal of **3**thf. An additional, small broad singlet at –4.03 ppm, which was repeatedly detected in [D_8]THF solutions of crystalline samples of **3**BEt_4, may arise from the presence of minor amounts of residual hydridoborate or borane species.[10h]

DFT Calculations

Quantum chemical calculations further support the structural formulations of **2** and **3**. Full DFT optimizations at the BP86-D/def2-TZVP level of theory gave an excellent agreement of the calculated and the experimentally determined structures (Table 1). The shortening of the Ru–H distance of **3** (1.556 Å) compared the Ru–H bonds of **2** (1.707 Å) may be attributed to the smaller coordination number and the cationic charge of the complex. In agree-

ment with the solid-state structures, complex **3** displays slightly longer Ru–C bonds (by 0.019–0.022 Å) than **2**. It is tempting to attribute this slight difference to a diminished bonding interaction between ruthenium and the carbene. In order to gain more insight into the bond energetics of **2** and **3**, we calculated the interaction energy between the IMe ligands and the fragments RuH_2 (**2**) and RuH^+ (**3**).[21] Indeed, the neutral complex **2** features a stronger interaction energy (–119.6 kcal mol^{-1} per IMe ligand) than cation **3** (–98.8 kcal mol^{-1} per IMe ligand). Furthermore, we performed NBO and NPA analyses on the optimized geometries of **2** and **3**. As expected the metal atom in **3** displays a more positive natural charge (–0.92) than in the neutral dihydride **2** (–1.62). The Ru–C bonding NBOs of neutral dihydride **2** show occupation numbers of 1.87 and 1.84 electrons. The corresponding NBO of cation **3** is only slightly less populated (1.82). The Ru–C bonds of **2** feature a Wiberg bond index of 0.85 while the Wiberg bond index for the Ru–C bonds of **3** is a slightly lower (0.82). Thus, the Ru–C bond strength in **3** appears to be slightly reduced compared to **2** although the observed differences are quite small. One possible explanation may be a reduction in metal–ligand backbonding in the cationic complex **3**. π-Backbonding has been discussed as a factor that potentially contributes to NHC transition metal bonds.[22] Future analyses must show whether such interactions are also significant in tetrakiscarbene hydridoruthenium complexes.

An interesting aspect of **2** is the *trans* arrangement of the hydrido ligands, which is in contrast to the *cis* geometry that is adopted by related phosphane complexes.[1] Optimization of the hypothetical *cis* dihydride *cis*-$[RuH_2(IMe)_4]$ (**2a**, Figure 3) showed that this complex is +14.3 kcal mol^{-1} higher in energy than *trans* complex **2**. Interestingly, the simplified models *cis*-$[RuH_2(Im)_4]$ (**2a′**, Figure 3) and *trans*-$[RuH_2(Im)_4]$ (**2′**) where the methyl substituents of the carbene ligands were replaced by hydrogen atoms, show practically no difference in energy. The methyl-substituted ligands (IMe) and parent imidazol-2-ylidene ligands (Im) have very similar electronic properties.[23] To investigate the possible influence of electronic effects further we optimized the complexes *trans*-$[RuH_2(aIm)_4]$ (**2′′**, Figure 3) and *cis*-$[RuH_2(aIm)_4]$ (**2a′′**), which contain the much more electron-donating "abnormal" carbenes imidazol-5-ylidene (aIm).[24] Again, we found practically no energy difference between **2′′** and **2a′′**. Thus, the preference for a *trans* structure is most likely of steric origin.

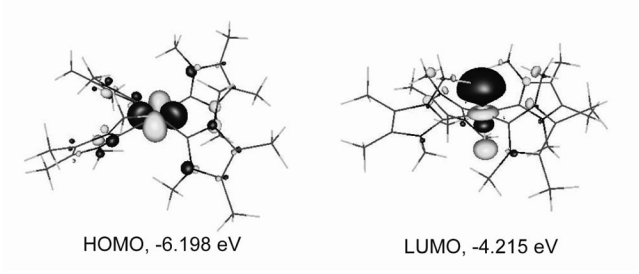

Figure 4. Frontier orbitals of **3**.

The frontier Kohn–Sham orbitals of $[RuH(IMe)_4]^+$ (**3**) are depicted in Figure 4. A Mulliken population analysis revealed that the HOMO displays 57% d character with the remaining contributions arising from ligand π orbitals. The LUMO represents an antibonding combination of a hydrogen s orbital (13% contribution according to the Mulliken analysis) and ruthenium s (5%), p (27%) and d orbitals (17%). According to its shape and low energy, the LUMO should be very well-suited for favorable interactions with donor orbitals from coordinating molecules.

Conclusions

Hydridoruthenium complexes *trans*-$[RuH_2(IMe)_4]$ (**2**) and $[RuH(IMe)_4][BEt_4]$ (**3**BEt_3), supported by four N-heterocyclic carbene ligands, are readily accessible by reaction of the chloro precursor *trans*-$[RuCl_2(IMe)_4]$ (**1**) with $LiAlH_4$ and $LiBHEt_3$, respectively. The special steric properties of the carbenes employed in this study favor the formation of a *trans* structure for **2**, whereas a *cis* arrangement is frequently observed for related phosphane complexes. The cationic complex **3** displays a sterically protected coordination site, opening up the interesting prospect of using **3** and related complexes for the binding and activation of small molecules.

Experimental Section

General: All procedures were carried out under an inert atmosphere of purified argon and in dried solvents (toluene, THF and diethyl ether with Na/benzophenone, *n*-hexane with $LiAlH_4$). $[RuCl_2(cod)]_x$ and IMe were prepared according to literature procedures.[25,26] $LiAlH_4$ was recrystallized from diethyl ether before use. The connectivity of the ligand atoms was confirmed using two-dimensional NMR spectroscopy (HMBC, NOESY).

Synthesis of 1: $[RuCl_2(cod)]_x$ (0.280 g, 1.00 mmol) and IMe (0.505 g, 4.00 mmol) were dissolved in toluene (60 mL) and heated to 100 °C for four hours. After cooling to room temperature, the reaction mixture was filtered and all volatile materials were removed in vacuo. The brown residue was washed with *n*-hexane and suspended in THF (40 mL). After filtration, the solution was layered with *n*-hexane (60 mL) to obtain **1** as an orange-brown solid. Crystals of **1** were grown at room temperature by layering a dilute THF solution with *n*-hexane. Yield 0.293 g (44%); m.p. (argon, sealed capillary) 263 °C (dec.). ^{1}H NMR (400 MHz, C_6D_6, 300 K): δ = 1.66 (s, 24 H, C*CH*$_3$), 3.55 (s, 24 H, N*CH*$_3$) ppm. ^{13}C NMR (101 MHz, C_6D_6, 300 K): δ = 9.7 (s, C*CH*$_3$), 35.4 (s, N*CH*$_3$), 124.0 (s, *CCH*$_3$), 198.7 (m, *C*Ru) ppm. MS (EI20 eV): *m*/*z* (%) = 544 (33) $[RuCl_2(IMe)_3^+]$, 420 (100) $[RuCl_2(IMe)_2^+]$. IR (KBr, nujol): $\tilde{\nu}$ = 457 (w), 1057 (s), 1153 (m), 2668 (w), 2721 (m) cm^{-1}. UV/Vis (THF, ε_{max}/dm^3 mol^{-1} cm^{-1}): λ_{max} = 288 (16500) nm. $C_{28}H_{48}Cl_2N_8Ru$ (668.7): calcd. C 50.3, H 7.2, N 16.8; found C 50.0, H 7.0, N 16.2.

Synthesis of 2: $[RuCl_2(IMe)_4]$ (**1**) (0.280 g, 0.45 mmol) and $LiAlH_4$ (0.035 g, 0.92 mmol) were dissolved in THF, and the mixture was stirred at room temperature for two days. Further $LiAlH_4$ (0.035 g, 0.92 mmol) was added and the reaction mixture was stirred at room temperature for another two days. After removing all volatile materials in vacuo, the yellow residue was washed with *n*-hexane and dissolved in diethyl ether (30 mL). After concentrating the solution

to 20 mL, yellow crystals of **2** were obtained at –18 °C which were contaminated with about 20% of a yellow, crystalline by-product that could not be separated, Yield 0.024 g (11% ref. to **2**); m.p. (argon, sealed capillary) 162 °C. ^{1}H NMR (400 MHz, C_6D_6, 300 K, product mixture): δ = –16.24 (s, 0.2 H, *H*Ru of by-product), –7.45 (s, 2 H, RuH_2 of **2**), 1.69 (s, 2.4 H, CCH_3 of by-product), 1.73 (s, 2.4 H, CCH_3 of by-product), 1.84 (s, 24 H, C*C*H$_3$ of **2**), 3.22 (s, 2.4 H, NCH_3 of by-product), 3.70 (s, 2.4 H, NCH_3 of by-product), 3.80 (s, 24 H, NCH_3 of **2**) ppm. ^{13}C NMR (101 MHz, C_6D_6, 300 K): δ = 9.5 (s, C*C*H$_3$ of by-product), 9.9 (s, C*C*H$_3$ of byproduct), 10.3 (s, C*C*H$_3$ of **2**), 35.0 (s, N*C*H$_3$ of by-product), 36.1 (s, N*C*H$_3$ of **2**), 37.2 (s, N*C*H$_3$ of by-product), 120.5 (s, *C*CH$_3$ of **2**), 121.9 (s, *C*CH$_3$ of by-product), 122.5 (s, *C*CH$_3$ of by-product), 200.9 (m, *C*Ru of by-product), 212.0 (m, *C*Ru of **2**) ppm. MS (MALDI-TOF, matrix DCTB): *m*/*z* = 599 ([RuH(IMe)$_4$]$^+$). IR (product mixture, KBr, nujol): $\tilde{\nu}$ = 667 (vw), 694 (w), 723 (m), 758 (s), 851 (vw), 1049 (m), 1070 (m), 1342 (w), 1365 (s), 1413 (w), 1713 (vw, $\nu_{Ru–H}$ of by-product), 1852 (w, $\nu_{Ru–H}$ of **2**) cm^{-1}.

Synthesis of 3BEt$_4$: LiBEt$_3$H (0.093 g, 0.88 mmol, 1 M solution in THF) was added dropwise to a solution of [RuCl$_2$(IMe)$_4$] (**1**) (0.293 g, 0.44 mmol) in THF. The color changed to deep violet on stirring overnight at room temperature. After filtration, all volatile materials were removed in vacuo and the residue was washed with *n*-hexane. The crude product was dissolved in THF (20 mL) and layered with *n*-hexane (20 mL) to yield **3** as deep violet crystals. Yield 0.074 g (23%); m.p. (argon, sealed capillary) 216 °C. ^{1}H NMR (400 MHz, fluorobenzene, 300 K): δ = –39.06 (br., 1 H, *H*Ru), 0.94 (br. m, 8 H, BCH_2CH$_3$), 1.58 (br. m, 12 H, BCH$_2$CH_3), 1.88 (s, 24 H, CCH_3), 3.21 (s, 12 H, NCH_3), 3.71 (s, 12 H, NCH_3) ppm. ^{1}H NMR (400 MHz, [D$_8$]THF, 300 K): δ = –40.1 (br., 0.25 H, *H*Ru), –0.17 (m, J_{H-11B} = 4.0, J_{H-10B} = 1.3, J_{H-H} = 7.8 Hz, 8 H, BCH_2CH$_3$), 0.61 (m, J_{H-11B} = 2.9, J_{H-10B} = 1.0, J_{H-H} = 7.8 Hz, 12 H, BCH$_2$CH_3), 2.04 (s, 24 H, CCH_3), 3.11 (s, 12 H, NCH_3), 3.13 (s, 12 H, NCH_3) ppm. ^{1}H NMR (400 MHz, [D$_8$]THF, 220 K): δ = –40.01 (s, 1 H, *H*Ru of **3**), –8.99 (s, 0.16 H, *H*Ru of **3**thf), –0.22 (m, 8 H, BCH_2CH$_3$), 0.61 (m, 12 H, BCH$_2$CH_3), 2.04 (s, 28 H, CCH_3 of **3** and **3**thf), 3.03 (s, 2 H, NCH_3 of **3**thf), 3.13 (overlapping s, 26 H, NCH_3 of **3** and **3**thf) ppm. ^{13}C{^{1}H} NMR (101 MHz, [D$_8$]-THF, 300 K): δ = 9.2 (s, C*C*H$_3$), 9.6 (s, C*C*H$_3$), 12.3 (s, J_{C-11B} = 13.7 Hz, BCH$_2$*C*H$_3$), 17.9 (q, $^1J_{C\ 11B}$ = 40.8 Hz, B*C*H$_2$CH$_3$), 34.0 (s, N*C*H$_3$), 34.4 (s, N*C*H$_3$), 123.6 (s, *C*CH$_3$), 123.9 (s, *C*CH$_3$), 200.9 (m, *C*Ru) ppm. ^{11}B NMR (128 MHz, [D$_8$]THF, 300 K): δ = –16.5 (br. s) ppm. MS (MALDI-TOF, matrix DCTB): *m*/*z* = 599 ([RuH(IMe)$_4$]$^+$). IR (KBr, nujol): $\tilde{\nu}$ = 843 (vw), 1055 (m), 1148 (w), 1352 (w), 2081 (w, $\nu_{Ru–H}$) cm^{-1}. UV/Vis (THF, ε_{max}/dm^3 mol^{-1} cm^{-1}): λ_{max} = 299 (3770), 562 (710) nm. $C_{36}H_{69}BN_8Ru$ (725.9): calcd. C 59.6, H 9.6, N 15.4; found C 59.3, H 9.5, N 15.6.

Crystal Structure Determinations: The crystallographic data were collected with a Bruker APEX diffractometer equipped with a rotating anode (Mo-K_α radiation). The crystals were coated with a perfluoro polyether, picked up with a glass fiber and immediately mounted in the cooled nitrogen stream of the diffractometer. Crystallographic data and details of the final refinement are provided in Table 2.[27] All non-hydrogen atoms were refined with anisotropic displacement parameters. The hydrogen atoms of **2** and **3** coordinated to ruthenium were located in the Fourier difference map and refined freely. The hydrogen atom H1 in **3** was disordered over two positions (50% occupancy each), but could be refined freely with a reasonable adp. All hydrogen atoms attached to carbon were calculated on ideal positions and allowed to ride on the bonded atom with U = 1.2 U_{eq}(C).

CCDC-739693 (for **1**), -739694 (for **2**), and -739695 (for **3**) contain the supplementary crystallographic data for this paper. These data can be obtained free of charge from The Cambridge Crystallographic Data Centre via www.ccdc.cam.ac.uk/data_request/cif.

DFT Calculations: Calculations based on Kohn–Sham density functional theory (DFT) have been carried out using the

Table 2. Crystal data and structural refinement for the complexes **1**–**3**BEt$_4$.[a]

	1	**2**	**3**BEt$_4$
Empirical formula	$C_{28}H_{48}Cl_2N_8Ru$	$C_{28}H_{50}N_8Ru$	$C_{36}H_{69}BN_8Ru$
Temperature [K]	153(2)	153(2)	153(2)
Crystal system	tetragonal	orthorhombic	orthorhombic
Space group	*P*4*nc*	*Fddd*	*Pcca*
a [Å]	11.9564(10)	21.4773(13)	21.1628(14)
b[Å]	11.9564(10)	23.5775(14)	10.6774(7)
c[Å]	10.8963(13)	25.4642(15)	17.6705(11)
α[°]	90	90	90
β[°]	90	90	90
γ [°]	90	90	90
V [10^{-30} m^3]	1557.7(3)	12894.6(13)	3992.9(4)
Z	2	16	4
$D_{calcd.}$ [g cm^{-3}]	1.426	1.236	1.207
μ [mm^{-1}]	0.707	0.515	0.427
Crystal size [mm]	0.05 × 0.03 × 0.02	0.15 × 0.02 × 0.02	0.18 × 0.15 × 0.01
Radiation		Mo-K_α, graphite-monochromator	
θ range for data collection [°]	4.41 < θ < 29.59	1.51 < θ < 26.00	1.91 < θ < 29.61
Index ranges	–16 ≤ *h* ≤ 16	–26 ≤ *h* ≤ 26	–29 ≤ *h* ≤ 28
	–16 ≤ *k* ≤ 16	–28 ≤ *k* ≤ 29	–14 ≤ *k* ≤ 14
	–14 ≤ *l* ≤ 15	–31 ≤ *l* ≤ 31	–24 ≤ *l* ≤ 24
Independent reflections	2197 (R_{int} = 0.0477)	3183 (R_{int} = 0.0440)	5629 (R_{int} = 0.0347)
Parameters	92	180	223
R = Σ||F_o| – |F_c||/|F_o| [F > 4σ (F)]	0.0279	0.0264	0.0270
wR_2 = w(|F_o| – |F_c|^2)^2	0.0695	0.0683	0.0808
Max./min. residual electron density [10^{30} em^{-3}]	0.453/–0.613	1.277/–0.420	0.396/–0.637

[a] Programs SHELXTL, SHELXTL-97;[27] solutions using the Patterson method, full-matrix refinement with all independent structure factors.

TURBOMOLE quantum chemical program system.[28] Full, unconstrained structural optimizations have been performed using large triple-ζ Gaussian AO basis sets (def2-TZVP) with effective core potential on ruthenium,[29] and the RI integral approximation has been employed.[30] As density functionals the BP86 functional has been used.[31] In all DFT treatments we used the now well-established correction for long-range London dispersion effects (DFT-D method).[32] Stationary points were identified as local minima by frequency calculations (no imaginary frequencies $>50\ cm^{-1}$) using the program AOFORCE.[33] A comparison of theoretical and experimental structural data for **2** and **3** is given in Table 1. NBO analyses[34] were performed using NBO version 3.1 implemented in Gaussian03.[35]

Supporting Information (see also the footnote on the first page of this article): Cartesian coordinates and energies of all calculated structures.

Acknowledgments

We thank Dr. C. Mück-Lichtenfeld, Prof. Dr. S. Grimme, Dr. M. Waller, Dr. U. Helmstedt, and Dr. J. J. Weigand for valuable discussions. Furthermore, we would like to thank the anonymous referees for helpful comments and suggestions. Prof. Dr. W. Uhl is thanked for his generous support. Financial support by the Fonds der Chemischen Industrie (Liebig fellowship for R. W.) and the Deutsche Forschungsgemeinschaft (DFG) (SFB858) is gratefully acknowledged.

[1] a) J. J. Levison, S. D. Robinson, *J. Chem. Soc. A* **1970**, 2947; b) M. T. Bautista, E. P. Cappellani, S. D. Drouin, R. H. Morris, C. T. Schweitzer, A. Sella, J. Zubkowski, *J. Am. Chem. Soc.* **1991**, *113*, 4876; c) A. Mezzetti, A. Del Zotto, P. Rigo, E. Farnetti, *J. Chem. Soc., Dalton Trans.* **1991**, 1525; d) B. Chin, A. J. Lough, R. H. Morris, C. T. Schweitzer, C. D′Agostino, *Inorg. Chem.* **1994**, *33*, 6278; e) S. P. Nolan, T. R. Belderrain, R. H. Grubbs, *Organometallics* **1997**, *16*, 5569; f) D. G. Gusev, R. Hübener, P. Burger, O. Orama, H. Berke, *J. Am. Chem. Soc.* **1997**, *119*, 3716, and ref. therein.

[2] Examples for catalytic applications: a) M. O. Albers, E. Singleton, M. M. Viney, *J. Mol. Catal.* **1985**, *33*, 77; b) M. Saburi, M. Ohnuki, M. T. Ogasawa, T. Takahashi, Y. Uchida, *Tetrahedron Lett.* **1992**, *33*, 5783; c) R. Noyori, S. Hashiguchi, *Acc. Chem. Res.* **1997**, *30*, 97; d) Y. Kayaki, H. Ikeda, J.-I. Tsurumaki, I. Shimizu, A. Yamamoto, *Bull. Chem. Soc. Jpn.* **2008**, *81*, 1053.

[3] a) M. Jiménez-Tenorio, M. C. Puerta, P. Valerga, *J. Am. Chem. Soc.* **1993**, *115*, 9794; b) M. Jiménez-Tenorio, M. C. Puerta, P. Valerga, *Inorg. Chem.* **1994**, *33*, 3515; c) M. Schlaf, A. J. Lough, R. H. Morris, *Organometallics* **1997**, *16*, 1253.

[4] J. G. Cordaro, D. Stein, H. Rüegger, H. Grützmacher, *Angew. Chem.* **2006**, *118*, 6305; *Angew. Chem. Int. Ed.* **2006**, *45*, 6159.

[5] Review: F. E. Hahn, M. C. Jahnke, *Angew. Chem.* **2008**, *120*, 3166; *Angew. Chem. Int. Ed.* **2008**, *47*, 3122.

[6] a) S. Burling, B. M. Paine, D. Nama, V. S. Brown, M. F. Mahon, T. J. Prior, P. S. Pregosin, M. K. Whittlesey, M. J. Williams, *J. Am. Chem. Soc.* **2007**, *129*, 1987; b) J. S. P. Reade, M. F. Mahon, M. K. Whittlesey, *J. Am. Chem. Soc.* **2009**, *131*, 1847.

[7] a) H. M. Lee, D. C. Smith Jr., Z. He, E. D. Stevens, C. S. Yi, S. P. Nolan, *Organometallics* **2001**, *20*, 794; b) R. F. R. Jazzar, S. A. Macgregor, M. F. Mahon, S. P. Richards, M. K. Whittlesey, *J. Am. Chem. Soc.* **2002**, *124*, 4944; c) S. L. Chatwin, R. A. Diggle, R. F. R. Jazzar, S. A. Macgregor, M. F. Mahon, M. K. Whittlesey, *Inorg. Chem.* **2003**, *42*, 7695; d) R. F. R. Jazzar, P. H. Bhatia, M. F. Mahon, M. K. Whittlesey, *Organometallics* **2003**, *22*, 670; e) D. Giunta, M. Holscher, C. W. Lehmann, R. Mynott, C. Wirtz, W. Leitner, *Adv. Synth. Catal.* **2003**, *345*, 1139; f) S. Burling, M. F. Mahon, B. M. Paine, M. K. Whittlesey, J. M. J. Williams, *Organometallics* **2004**, *23*, 4537; g) K. Abdur-Rashid, T. Fedorkiw, A. J. Lough, R. H. Morris, *Organometallics* **2004**, *23*, 86; h) S. Burling, G. Kociok-Köhn, M. F. Mahon, M. K. Whittlesey, J. M. J. Williams, *Organometallics* **2005**, *24*, 5868; i) S. L. Chatwin, M. G. Davidson, C. Doherty, S. M. Donald, R. F. R. Jazzar, S. A. Macgregor, G. J. McIntyre, M. F. Mahon, M. K. Whittlesey, *Organometallics* **2006**, *25*, 99; j) S. P. Reade, D. Nama, M. F. Mahon, P. S. Pregosin, M. K. Whittlesey, *Organometallics* **2007**, *26*, 3484; k) R. A. Diggle, S. A. Macgregor, M. K. Whittlesey, *Organometallics* **2008**, *27*, 617; l) V. L. Chandler, S. L. Chatwin, R. F. R. Jazzar, M. F. Mahon, O. Saker, M. K. Whittlesey, *Dalton Trans.* **2008**, 2603; m) L. J. L. Häller, M. J. Page, S. A. Macgregor, M. F. Mahon, M. K. Whittlesey, *J. Am. Chem. Soc.* **2009**, *131*, 4604.

[8] S. Burling, M. F. Mahon, R. E. Powell, M. K. Whittlesey, J. M. J. Williams, *J. Am. Chem. Soc.* **2006**, *128*, 13702.

[9] a) Homoleptic CNC-Pincer Carbene Complex: M. Poyatos, M. A. Mata, E. Falomir, R. H. Crabtree, E. Peris, *Organometallics* **2003**, *22*, 1100; b) L. J. L. Häller, E. Mas-Marzá, A. Moreno, J. P. Lowe, S. A. Macgregor, M. F. Mahon, P. S. Pregosin, M. K. Whittlesey, *J. Am. Chem. Soc.* **2009**, *131*, 9518; c) S. Burling, L. J. L. Häller, E. Mas-Marzá, A. Moreno, S. A. Macgregor, M. F. Mahon, P. Pregosin, M. K. Whittlesey, *Chem. Eur. J.* **2009**, *15*, 10923.

[10] a) G. Smith, D. J. Cole-Hamilton, *J. Chem. Soc., Chem. Commun.* **1982**, 490; b) G. Smith, D. J. Cole-Hamilton, *J. Chem. Soc., Dalton Trans.* **1983**, 2501; c) E. Thaler, K. Folting, J. C. Huffman, K. G. Caulton, *Inorg. Chem.* **1987**, *26*, 374; d) D. Carmichael, P. B. Hitchcock, J. F. Nixon, A. Pidcock, *J. Chem. Soc., Chem. Commun.* **1988**, 1555; e) M. D. Fryzuk, B. R. Lloyd, G. K. Clentsmith, S. J. Rettig, *J. Am. Chem. Soc.* **1991**, *113*, 4332; f) M. D. Fryzuk, B. R. Lloyd, G. K. Clentsmith, S. J. Rettig, *J. Am. Chem. Soc.* **1994**, *116*, 3804; g) T. S. Cameron, M. E. Peach, *J. Chem. Crystallogr.* **1998**, *28*, 919; h) M. G. Crestani, M. Muñoz-Henández, A. Arévalo, A. Acosta-Ramirez, J. J. García, *J. Am. Chem. Soc.* **2005**, *127*, 18066.

[11] $LiBHEt_3$ [$\delta(^{11}B)$ = 12,3] forms an equilibrium with $LiBEt_2H_2$ and $LiBEt_4$: H. C. Brown, E. J. Mead, C. J. Short, *J. Am. Chem. Soc.* **1956**, *78*, 3616.

[12] Search in the CSD database, version 5.30, november **2008**: Ru–C bond lengths of 181 complexes containing a RuCl(NHC) fragment range from 1.908 to 2.168 Å (average 2.047 Å); Ru–Cl distances range from 2.261 to 2.532 Å (average: 2.395 Å).

[13] The sum of the van-der-Waals radii of Cl and Me is 3.75 Å; cf. A. Bondi, *J. Phys. Chem.* **1964**, *68*, 441.

[14] P. B. Hitchcock, M. F. Lappert, P. L. Pye, *J. Chem. Soc., Dalton Trans.* **1978**, 826.

[15] Similar Ru–H distances have been determined by neutron diffraction for $[CpRuH(PMe_3)]$ [Ru–H 1.630(4) Å] and $[CpRuH_2(PMe_3)]BF_4$ [Ru–H 1.599(8) and 1.604(9) Å]; L. Brammer, W. T. Klooster, F. R. Lemke, *Organometallics* **1996**, *15*, 1721.

[16] Search in the CSD database, version 5.30, november **2008**: Ru–H bond lengths of 38 complexes containing a RuH(NHC) fragment range from 1.444 to 1.668 Å (average 1.595 Å); Ru–C distances range from 1.967 to 2.192 Å (average: 2.099 Å).

[17] The distances between the methyl carbons of this pocket (C4, C5, C11, C12) range from 3.965 to 5.684 Å.

[18] R. Boese, D. Bläser, N. Niederblüm, M. Nüsse, W. A. Brett, P. von Ragué Schleyer, M. Bühl, M. J. R. van Eikema Hommes, *Angew. Chem.* **1992**, *104*, 356; *Angew. Chem. Int. Ed. Engl.* **1992**, *31*, 314.

[19] H. Salem, L. J. W. Shimon, Y. Diskin-Posner, G. Leitus, Y. Ben-David, D. Milstein, *Organometallics* **2009**, *28*, 4791.

[20] Adducts $[RuH(dippe)_2L][BPh_4]$ (L = CO, CN*t*Bu, CH_3CN) display similar high-field shifts compared to uncoordinated $[RuH(dippe)_2L]$ as observed for **3**; see ref.[3b]

[21] Single-point calculations were performed on the fragments RuH_2, RuH^+ and IMe_4 using coordinates obtained from the optimized geometries of **2** and **3**. The interaction energies E_{int} were calculated by subtracting these single-point energies from the total energies of the complete molecules **2** and **3**: E_{int}(**2**) = E_{total}(**2**) – E(RuH_2) – E(IMe_4 of **2**), E_{int}(**3**) = E_{total}(**3**) – E(RuH^+) – E(IMe_4 of **3**); cf. the Supporting Information
[22] a) X. Hu, I. Castro-Rodriguez, K. Olsen, K. Meyer, *Organometallics* **2004**, *23*, 755; b) U. Radius, F. M. Bickelhaupt, *Organometallics* **2008**, *27*, 3410.
[23] Changes in the substituent patterns of NHCs generally effect only minor differences in their donor properties: a) R. Dorta, E. D. Stevens, N. M. Scott, C. Costabile, L. Cavallo, C. D. Hoff, S. P. Nolan, *J. Am. Chem. Soc.* **2005**, *127*, 2485; b) R. H. Crabtree, *J. Organomet. Chem.* **2005**, *690*, 5451.
[24] Cf. the Supporting Information
[25] a) M. A. Bennett, G. Wilkinson, *Chem. Ind.* **1959**, 1516; b) M. O. Albers, T. V. Ashworth, E. Oosthuizen, E. Singleton, *Inorg. Synth.* **1989**, *26*, 68.
[26] N. Kuhn, T. Kratz, *Synthesis* **1992**, 561.
[27] *SHELXTL-Plus*, rel. 4.1, Siemens Analytical X-RAY Instruments Inc., Madison, WI, **1990**, G. M. Sheldrick, *SHELXL 97*, Program for the Refinement of Structures, University of Göttingen, **1997**.
[28] R. Ahlrichs, F. Furche, C. Hättig, W. Klopper, M. Sierka, F. Weigend, *TURBOMOLE*, *Version 5.9*; University of Karlsruhe, Karlsruhe, Germany, **2006**; http://www.turbomole.com.
[29] a) F. Weigend, R. Ahlrichs, *Phys. Chem. Chem. Phys.* **2005**, *7*, 3297; b) D. Andrae, U. Haeussermann, M. Dolg, H. Stoll, H. Preuss, *Theor. Chim. Acta* **1990**, *77*, 123.
[30] a) K. Eichkorn, O. Treutler, H. Oehm, M. Häser, R. Ahlrichs, *Chem. Phys. Lett.* **1995**, *242*, 652; b) K. Eichkorn, F. Weigend, O. Treutler, R. Ahlrichs, *Theor. Chem. Acc.* **1997**, *97*, 119.
[31] a) A. D. Becke, *Phys. Rev. A* **1988**, *38*, 3089; b) J. P. Perdew, *Phys. Rev. B* **1986**, *33*, 8822; c) J. P. Perdew, *Phys. Rev. B* **1986**, *33*, 7406.
[32] S. Grimme, *J. Comput. Chem.* **2006**, *27*, 1787.
[33] P. Denglmann, K. May, F. Furche, R. Ahlrichs, *Chem. Phys. Lett.* **2004**, *384*, 103.
[34] F. Weinhold, C. Landis, *Valency and Bonding*, Cambridge University Press, **2005**.
[35] M. J. Frisch, G. W. Trucks, H. B. Schlegel, G. E. Scuseria, M. A. Robb, J. R. Cheeseman, J. A. Montgomery, Jr., T. Vreven, K. N. Kudin, J. C. Burant, J. M. Millam, S. S. Iyengar, J. Tomasi, V. Barone, B. Mennucci, M. Cossi, G. Scalmani, N. Rega, G. A. Petersson, H. Nakatsuji, M. Hada, M. Ehara, K. Toyota, R. Fukuda, J. Hasegawa, M. Ishida, T. Nakajima, Y. Honda, O. Kitao, H. Nakai, M. Klene, X. Li, J. E. Knox, H. P. Hratchian, J. B. Cross, V. Bakken, C. Adamo, J. Jaramillo, R. Gomperts, R. E. Stratmann, O. Yazyev, A. J. Austin, R. Cammi, C. Pomelli, J. W. Ochterski, P. Y. Ayala, K. Morokuma, G. A. Voth, P. Salvador, J. J. Dannenberg, V. G. Zakrzewski, S. Dapprich, A. D. Daniels, M. C. Strain, O. Farkas, D. K. Malick, A. D. Rabuck, K. Raghavachari, J. B. Foresman, J. V. Ortiz, Q. Cui, A. G. Baboul, S. Clifford, J. Cioslowski, B. B. Stefanov, G. Liu, A. Liashenko, P. Piskorz, I. Komaromi, R. L. Martin, D. J. Fox, T. Keith, M. A. Al-Laham, C. Y. Peng, A. Nanayakkara, M. Challacombe, P. M. W. Gill, B. Johnson, W. Chen, M. W. Wong, C. Gonzalez, J. A. Pople, *Gaussian 03, Revision E.01*, Gaussian, Inc., Wallingford, CT, **2004**.

Received: July 24, 2009
Published Online: January 8, 2010

